Carcinogenesis, 2019, Vol. 40, No. 1, 164–172

doi:10.1093/carcin/bgy131
Advance Access publication October 6, 2018
Original Article

ORIGINAL ARTICLE

RAD9A promotes metastatic phenotypes through transcriptional regulation of anterior gradient 2 (AGR2)

Constantinos G. Broustas[1], Kevin M. Hopkins[1], Sunil K. Panigrahi[1], Li Wang[1], Renu K. Virk[2] and Howard B. Lieberman[1,3,*]

[1]Center for Radiological Research, Columbia University Vagelos College of Physicians and Surgeons, [2]Department of Pathology and Cell Biology and [3]Department of Environmental Health Sciences, Mailman School of Public Health, Columbia University Irving Medical Center, New York, NY 10032, USA

*To whom correspondence should be addressed. Center for Radiological Research, Columbia University Vagelos College of Physicians and Surgeons, 630 W. 168th St., New York, NY 10032, USA. Email: HBL1@cumc.columbia.edu

Abstract

RAD9A plays an important role in prostate tumorigenesis and metastasis-related phenotypes. The protein classically functions as part of the RAD9A-HUS1-RAD1 complex but can also act independently. RAD9A can selectively transactivate multiple genes, including *CDKN1A* and *NEIL1* by binding p53-consensus sequences in or near promoters. RAD9A is overexpressed in human prostate cancer specimens and cell lines; its expression correlates with tumor progression. Silencing RAD9A in prostate cancer cells impairs their ability to form tumors *in vivo* and migrate as well as grow anchorage independently *in vitro*. We demonstrate herein that RAD9A transcriptionally controls *AGR2*, a gene aberrantly overexpressed in patients with metastatic prostate cancer. Transient or stable knockdown of *RAD9A* in PC-3 cells caused downregulation of AGR2 protein abundance. Reduced AGR2 protein levels were due to lower abundance of *AGR2* mRNA. The *AGR2* genomic region upstream of the coding initiation site contains several p53 consensus sequences. RAD9A bound specifically to the 5′-untranslated region of *AGR2* in PC-3 cells at a partial p53 consensus sequence at position +3136 downstream from the transcription start site, determined by chromatin immunoprecipitation, followed by PCR amplification. Binding of RAD9A to the p53 consensus sequence was sufficient to drive *AGR2* gene transcription, shown by a luciferase reporter assay. In contrast, when the RAD9A-binding sequence on the *AGR2* was mutated, no luciferase activity was detected. Knockdown of RAD9A in PC-3 cells impaired cell migration and anchorage-independent growth. However, ectopically expressed *AGR2* in RAD9A-depleted PC-3 cells restored these phenotypes. Our results suggest RAD9A drives metastasis by controlling AGR2 abundance.

Introduction

Despite successes in treating localized primary prostate tumors, metastatic prostate cancer poses a real challenge. It remains essentially incurable and current therapeutic strategies extend overall patient survival by a few months (1, 2).

RAD9A is a pleiotropic protein involved in many aspects of DNA damage and repair (3). As part of the RAD9A-HUS1-RAD1 (9-1-1) complex, it acts as a sensor of DNA damage that enables ATR kinase, independently recruited to the site of damage, to phosphorylate and activate its downstream effector CHK1. Besides its role as part of the 9-1-1 complex, RAD9A can operate independently as a sequence-specific transcription factor. RAD9A is able to transactivate a select set of genes, including *CDKN1A* ($p21^{waf1/cip1}$) (4) and *NEIL1* (Nei-like DNA glycosylase 1), a DNA glycosylase involved in base excision repair (5). RAD9A regulates *CDKN1A* and *NEIL1* gene expression by binding to DNA sequences that are p53 response elements (6).

Aberrant RAD9A expression has been associated with prostate, breast, lung, skin, thyroid and gastric cancers (7). We demonstrated that RAD9A is overexpressed in human prostate cancer specimens, as well as prostate cancer cell lines (8).

Received: August 3, 2018; Revised: September 17, 2018; Accepted: October 4, 2018

Abbreviations

ChIP	chromatin immunoprecipitation
CRISPR	clustered regularly interspaced short palindromic repeats
ER	endoplasmic reticulum
gRNA	guide RNAs

Experiments designed to assess the contribution of RAD9A to prostate tumor growth revealed that downregulation of *RAD9A* in human prostate cancer cell line xenografts impairs growth in nude mice. Furthermore, immunohistochemical analysis of normal and tumor prostate specimens showed that RAD9A protein abundance increased along with advancement of cancer stage, suggesting a role for RAD9A in prostate malignant progression (8). *In vitro* evidence revealed that RAD9A downregulation impairs anchorage-independent growth, suppresses migration and invasion and sensitizes prostate cancer cell lines to anoikis, a form of apoptosis that epithelial cells activate when they lose attachment to an extracellular matrix (9). Conversely, expression of *Mrad9*, the mouse homolog, restores these cancer phenotypes. Although the role of RAD9A in DNA damage response and repair is well documented, it is unclear how this protein enhances prostate tumor progression and metastasis. Moreover, the nature of RAD9A effectors responsible for the tumorigenic/metastatic functions is poorly understood.

Anterior gradient protein 2 (AGR2) belongs to the protein disulfide isomerase family. Protein disulfide isomerase family members are defined by the presence of one or more thioredoxin domains containing the CXXC motif, and they catalyze formation of cysteine disulfide bonds critical for proper protein folding in the endoplasmic reticulum (ER) (10). Depending on the redox state of the protein disulfide isomerase, these CXXC motifs can mediate formation or reduction of disulfides in client proteins in the ER. AGR2 contains a thioredoxin fold structure (11). However, AGR2 contains only one active cysteine (CXXS motif), which does not allow it to transfer oxidizing equivalents to client proteins. However, this deficiency can be compensated by the ability of AGR2 to form homodimers, which can facilitate the bivalent transfer of oxidizing equivalents (11).

The *AGR* gene family consists of three members *AGR1*, *AGR2* and *AGR3* (10). Although *AGR1* has not been associated with cancer, *AGR2* and *AGR3* act as pro-oncogenic agents in various cancers, including of the breast and prostate. Human AGR2 protein is found in various cellular compartments, such as the ER, the nucleus, the cell surface and the extracellular matrix. Studies using AGR2 knockout cells have demonstrated that loss of the protein results in apparent fragmentation of the ER, suggesting that AGR2 has a significant impact on cellular homeostasis (12).

Overproduction of AGR2 promotes cellular transformation, cell migration and invasion, as well as transcriptional silencing of p53 in response to DNA damage (10). Mechanistically, AGR2 suppresses p53 activation through inhibition of p38 mitogen-activated protein kinase (13). AGR2 is markedly elevated in a majority of tumors, including prostate carcinoma. High expression of AGR2 has been associated with poor survival in lung adenocarcinoma patients (14). In regards to prostate cancer, aberrant *AGR2* mRNA and protein levels are detected in patients with metastatic disease (15). Furthermore, *AGR2* mRNA was initially discovered to be androgen inducible (16). However, AGR2 is also expressed at high levels in castration-resistant prostate cancer cell lines, suggesting that *AGR2* can be induced by both androgen/androgen-receptor-dependent and independent pathways.

Besides the intracellular localization of AGR2, cancer cells secrete the protein to the extracellular matrix. Secretion of AGR2 confers tumorigenic properties (17) and increased tumor cell survival (18). It is also associated with tumor progression (10). In addition, cancer-secreted AGR2 induces programmed cell death in normal cells (19). Finally, it has been proposed that serum AGR2 could be a useful cancer biomarker, such as for pituitary adenocarcinomas (20).

In this study, we show that RAD9A controls *AGR2* mRNA and protein levels. RAD9A binds at a partial p53-consensus sequence at the 5′-untranslated region of *AGR2* and regulates its expression. Silencing of RAD9A impairs cell migration and anchorage-independent cell growth, which is reversed by concomitantly expressing *AGR2*. These results further establish RAD9A as a pleiotropic transcription factor that has a significant role in tumor metastasis.

Materials and methods

Cell culture

Prostate cancer cells PC-3 and DU145 were purchased from ATCC (Manassas, VA) and no further authentication was performed. Cells for experiments were obtained from the original stock preserved in liquid nitrogen and they were passaged for <6 months. Both cell lines were grown at 37°C, 5% CO_2 in RPMI 1640 (Thermo Fisher), supplemented with 10% fetal bovine serum (Atlanta Biologicals or Thermo Fisher), 100 U/ml penicillin, 100 µg/ml streptomycin and 2.5 µg/ml Fungizone (Thermo Fisher).

RNA interference and plasmid construction

The pSUPER.retro.puro *RAD9A* shRNA expression vector (Oligoengine) and viral production have been described (9). We isolated two clones of PC-3 cells that stably downregulate *RAD9A*. Downregulation of RAD9A protein was assessed by western blotting with RAD9A antibody (BD Biosciences).

RNA interference experiments were carried out with siRNA against *RAD9A* (two non-overlapping siRNAs denoted 1 and 2), whereas *Luciferase* (siLuc) served as control. The sequences and concentrations of these siRNA have been reported (9). For transient transfection, cells at approximately 30% confluency were transfected with the indicated siRNA using Lipofectamine 3000 (Invitrogen), and protein abundance was examined 48–72 h later by western blot analysis.

MYC-DDK-tagged *AGR2* cDNA cloned into pCMV6 expression vector was purchased from OriGene. To isolate stable clones of PC-3/crRAD9A cells with AGR2, cells were transfected with *AGR2-MYC-DDK* plasmid, and colonies (#2, #6) were picked after 2–3 weeks of selection in 1 mg/ml G418.

The FLAG-tagged *RAD9A* cDNA was generated from mRNA extracted from PC-3 cells and reverse transcribed using a SuperScript III kit (Invitrogen). cDNA was amplified using PCR human *RAD9A* gene primers: forward, 5′-GGTACT*GGATCCATGGAT TACAAGGATGACGACGATAAGATGA* AGTGCCTGGTCACGGGCGGCA-3′ (BamHI underlined; FLAG-tag in italics) and reverse, 5′-GGTAGAC*TC GAGTCAGGCTTCACCC* TCACTGTCTTCCGC CAGCACAGGGCT-3′ (XhoI underlined). PCR conditions were 94°C for 2 min, 30 cycles of denaturation at 94°C for 30 s, annealing and extension at 68°C for 4 min and a final extension at 72°C for 7 min. The PCR-amplified product was ligated into the pcDNA3 expression vector (Invitrogen).

Generation of RAD9A knockout human prostate cancer cell lines with clustered regularly interspaced short palindromic repeats (crRAD9A)

Three *RAD9A* guide RNAs (gRNA) were designed using the software from Zhang Feng's lab at Massachusetts Institute of Technology (MIT) (http://crispr.mit.edu). The sequence of *RAD9A* gRNAs was 5′-GGTCACGGGCGGCAACGTGA-3′. The gRNA was used to target exon 1 of *RAD9A* at the fifth amino acid from the start codon. This gRNA was ligated to its complementary strand and cloned into lentiCRISPR v2 (Addgene # 52961) vector at BsmbI restriction site and confirmed by sequencing. Lentiviral particles with gRNA were produced in HEK293 cells as described

(4). After drug selection and isolation of single colonies, ~48 colonies for each cell line were tested for RAD9A protein levels by western blotting with anti-RAD9A antibodies. Two clones (#32, #41) showing minimum expression of RAD9A protein were chosen. RAD9A exon 1 covering the targeted gRNA region was amplified in both clones, inserted into PCR 2.1-TOPO-TA vector, and the sequences were determined.

Real-time quantitative PCR

TRIzol reagent (Invitrogen) was used to isolate RNA. One microgram of RNA was reverse transcribed to cDNA using the Superscript III transcriptase First Strand Synthesis System (Invitrogen). Real-time PCR was carried out in triplicate using SYBR-Green PCR Master Mix on the Vii7 Real-Time PCR instrument. Expression levels were normalized to *GAPDH* abundance. Analysis of relative gene expression was performed, using the $2^{-\Delta\Delta CT}$ method (21). The following sense and antisense primers were synthesized by Thermo Fisher: *AGR2*, 5′-GTCAGCATTCTTGCTCCTTGT-3′ (forward); 5′-GGGTCGAGAGTCCTTTGTGTC-3′ (reverse), *GAPDH*, 5′-CATCTCTG CCCCCTCTGCTG-3′ (forward) and 5′-CCCTCCGACGCCTGCTTCAC-3′ (reverse). Primers were designed using the PrimerBank resource (http://pga.mgh.harvard.edu/primerbank) (22).

Western blot analysis

Cells were lysed in radioimmune precipitation assay buffer, as described earlier (9). Protein was subjected to 4–12% Bis/Tris (Invitrogen) gel electrophoresis. Quantitation of band intensity was performed with ImageJ software v1.47f (http://rsb.info.nih.gov/ij/). The following antibodies were used in this study: RAD9A monoclonal antibodies (BD Biosciences #611324), AGR2 polyclonal antibodies (Abcam # ab76473), β-actin (#A1978) and α-tubulin (#T9026) monoclonal antibodies (Sigma).

Chromatin immunoprecipitation

Chromatin immunoprecipitation (ChIP) was performed as described by Panigrahi *et al.* (23), except with minor modifications. Chromatin from approximately 10^7 PC-3 cells was cross-linked by adding 1% formaldehyde for 10 min at room temperature; then the reaction was stopped by addition of 125 mM of glycine. The chromatin template was subsequently fragmented to a size of 150–200 bp by sonication. Debris was removed by centrifugation at 16 000× *g* for 10 min at 4°C. Aliquots of the chromatin samples were subjected to ChIP using an anti-RAD9A (Abcam #ab70810) antibody or rabbit IgG (Vector Laboratories # I-1000) as a control. Samples were then washed extensively and bound nucleoprotein complexes were eluted in 200 µl of elution buffer [50 mM Tris–HCl (pH 8.0), 10 mM ethylenediaminetetraacetic acid, 1% sodium dodecyl sulfate] at 65°C for 20 min. After elution, samples were incubated at 65°C for 12 h to reverse cross-links. The DNA was purified using the Qiagen PCR purification kit and served as template for PCR employing SYBR-Green PCR master mix (Applied Biosystems) in an ABI 7300 real-time PCR system, as per the manufacturer's instructions. Five primer pairs spanning the genomic region upstream of the *AGR2* initiation site were used. Primer sequences are listed in Supplementary Table 1, available at *Carcinogenesis* Online. The TRANSFAC database on transcription factors was used to predict p53-consensus binding sites (24).

Luciferase assay

PC-3/crRAD9A cells, lacking endogenous RAD9A, were transfected with 0.5 µg of Renilla luciferase reporter plasmid (pGL3; Promega), along with 2 µg of firefly luciferase reporter under the control of a wild-type sequence that conforms to a partial p53-consensus site or three different mutated genomic sequences upstream of the *AGR2* initiation site sequences (Supplementary Table 2, available at *Carcinogenesis* Online), and 2 µg of FLAG-RAD9A-pcDNA3 or empty expression vector using Lipofectamine 3000. Cell lysates were prepared 24 h later using the Dual Luciferase Assay System (Promega), according to the manufacturer's instructions. Firefly luciferase activity was determined by a Synergy 2 luminometer (BioTek) and normalized to Renilla luciferase activity.

Wound-healing assay

For the wound-healing migration assay, cell populations grown to confluency in 6-well plates were scratched with a sterile P200 pipette tip. Detached cells were removed with Dulbecco's phosphate-buffered saline. Attached cells were allowed to migrate in serum-free medium (RPMI/0.1% bovine serum albumin). Photographs of the wounds were taken at 0, 24, and 48 h after medium was added. The wound gap was quantified by National Institutes of Health ImageJ software (http://rsbweb.nih.gov/ij/).

Anchorage-independent growth assay

Cells were suspended in 500 µl of RPMI/10% fetal bovine serum medium containing 0.33% agarose and plated in duplicate on top of 1 ml of solidified 0.67% agarose/RPMI/10% fetal bovine serum in 12-well plates (1000 cells/well). Cells were placed in a 37°C and 5% CO_2 incubator, and colonies were allowed to form for 2 weeks. Colonies were stained with 0.005% crystal violet for 2 h, and photographs of five fields/well were taken under the microscope. Colonies with a diameter >20 µm were scored.

Statistical Analysis

Data were represented as mean ± standard deviation (S.D.). P values were calculated by a paired two-sided Student's t-test, and values < 0.05 were considered statistically significant.

Results

RAD9A controls AGR2 protein and mRNA levels

RAD9A promotes cell migration and invasion of DU145 and PC-3 human prostate cancer cells (9). Likewise, AGR2 has been identified recently as a pro-metastatic protein in a number of human malignancies, including prostate cancer (10). Preliminary results showed that *AGR2* is abundantly expressed in PC-3 cells, but barely in DU145 cells (Supplementary Figure 1, available at *Carcinogenesis* Online). Therefore, to test whether RAD9A and AGR2 are functionally related, we focused our studies on PC-3 cells. Initially, we transiently silenced *RAD9A* in PC-3 and examined AGR2 protein levels. Immunoblot analysis revealed that AGR2 abundance was significantly diminished in PC-3 treated with two different *RAD9A* siRNAs (Figure 1A and B). The average percent downregulation of AGR2 in response to transient *RAD9A* knockdown was approximately 60% for both RAD9A-1 ($P < 0.008$; $n = 3$) and RAD9A-2 ($P < 0.004$; $n = 3$). In contrast, *AGR2* silencing did not affect RAD9A protein levels (see Figure 5A). Furthermore, stable *RAD9A* knockdown by short hairpin (sh)RNA in two clones of PC-3 cells achieved a complete reduction of AGR2 protein (Figure 1C). Likewise, two independent PC-3 clones (#32, #41) with *RAD9A* knockout using clustered regularly interspaced short palindromic repeats (CRISPR)/Cas9 editing led to complete AGR2 downregulation (Figure 1D).

Next, we sought to determine whether *AGR2* mRNA expression is under the control of RAD9A, as it has been documented that RAD9A functions as a transcription factor. Quantitative real-time PCR showed that transient *RAD9A* knockdown using two independent siRNAs led to a 64% (RAD9A-1; $P < 0.002$; $n = 5$) and 53% (RAD9A-2; $P = 6.58E-05$; $n = 5$) downregulation of *AGR2* mRNA compared with cells expressing control luciferase siRNA (Figure 2A). Stable RAD9A downregulation in two clones of PC-3 cells resulted in complete reduction of *AGR2* mRNA compared with control insertless shRNA vector (Figure 2B). Finally, we demonstrate that *RAD9A* knockout (crRAD9A) reduces *AGR2* mRNA expression by more than 90% when compared with parental PC-3 cells (Figure 2C).

RAD9A binds directly to a sequence at the 5′-untranslated region of *AGR2* and drives its transcription

Previously, we showed that RAD9A functions as a transcription factor and binds to p53-consensus sequences at the promoter of

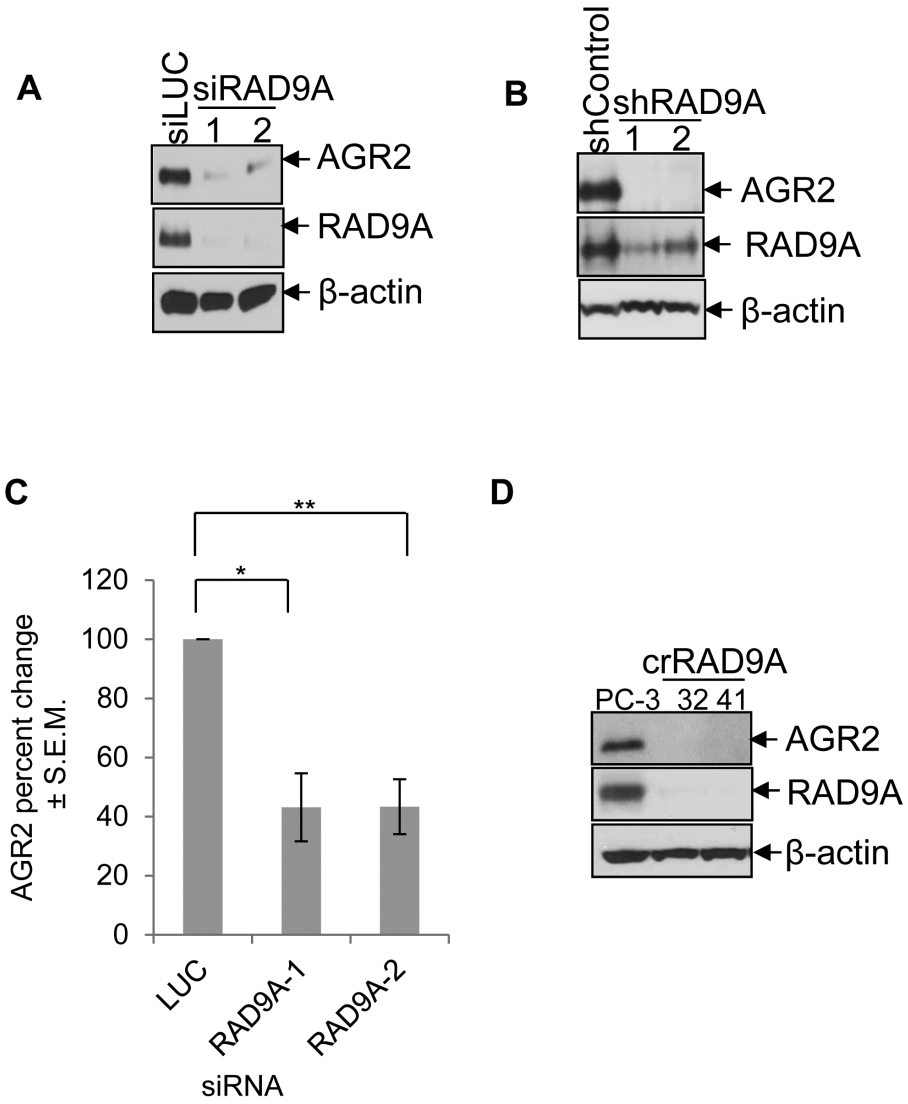

Figure 1. RAD9A knockdown reduces AGR2 protein levels. (**A**) PC-3 cells were transiently transfected with control (luciferase; *Luc*) or two non-overlapping *RAD9A* siRNAs (1, 2). Three days post-transfection, cell lysates were analyzed for AGR2, RAD9A and β-actin (loading control) protein levels by immunoblotting. (**B**) Cumulative data from three independent transfection experiments, as per part A. Data shown as mean ± SEM (n = 3). (**C**) PC-3 cells were stably transfected with either control (insertless pSUPER-retro vector) or *RAD9A* shRNA (two clones 1 and 2) and cell lysates were analyzed for AGR2, RAD9A and β-actin (loading control) protein levels by immunoblotting. * $P < 0.008$ (n =3); ** $P < 0.004$ (n = 3). EV, empty vector. (**D**) Western blot analysis of AGR2 and RAD9A abundance in RAD9A-CRISPR (crRAD9A) PC-3 cells (clones 32 and 41). β-actin is the loading control.

genes, such as $p21^{waf1/cip1}$ and *NEIL1* (4,5). Because RAD9A silencing reduced *AGR2* mRNA abundance, we reasoned that RAD9A may bind at or near the *AGR2* promoter and control gene transcription. Furthermore, we searched for p53-consensus sequences on the *AGR2* that could serve as candidates for RAD9A binding. We found that the *AGR2* contains several putative p53-consensus sequences within the –2000/+4000 bp region (Figure 3A and Supplementary Table 2, available at *Carcinogenesis* Online). To determine whether RAD9A bound any of these sequences, we performed ChIP-qPCR analysis. Our results showed that RAD9A selectively bound to an *AGR2* region at position +3136 (designated E-region), relative to the transcriptional start site, and it contained an imperfect p53-consensus sequence (Figure 3B).

Next, to assess the functionality of the binding, we cloned a ~4 kb fragment (–630 to +3212) of the human *AGR2* gene that contained the p53 consensus sequence at position +3136, into a luciferase (LUC) expression vector and co-transfected the 4 kb *AGR2-LUC* plasmid with the *CMV-RAD9A* expression vector into PC-3 cells knocked out for the inherent *RAD9A* gene (PC-3 crRAD9 #41 cells). Ectopically expressed RAD9A increased the transcriptional activity of the *AGR2*, as indicated by the high levels of luciferase activity detected (compare Figure 4A, columns 1 and 5). Site-directed mutagenesis of RAD9A binding sequences using two constructs with two different point mutations and a deletion construct (Supplementary Table 3, available at *Carcinogenesis* Online) blocked the ability of RAD9A to activate *AGR2* (Figure 4A, columns 2, 3 and 4), indicating that the F-region on the *AGR2* region upstream of the initiation site, where RAD9A binds, is required for RAD9A-directed activation of *AGR2* gene. Figure 4B shows that approximately equal amounts of FLAG-tagged RAD9A protein are present in the PC-3 crRAD9 #41 cells also containing wild-type or mutated versions of the *AGR2* putative p53 binding sites. The empty vector (pcDNA3 devoid of an insert) was transfected into the same cells as a control.

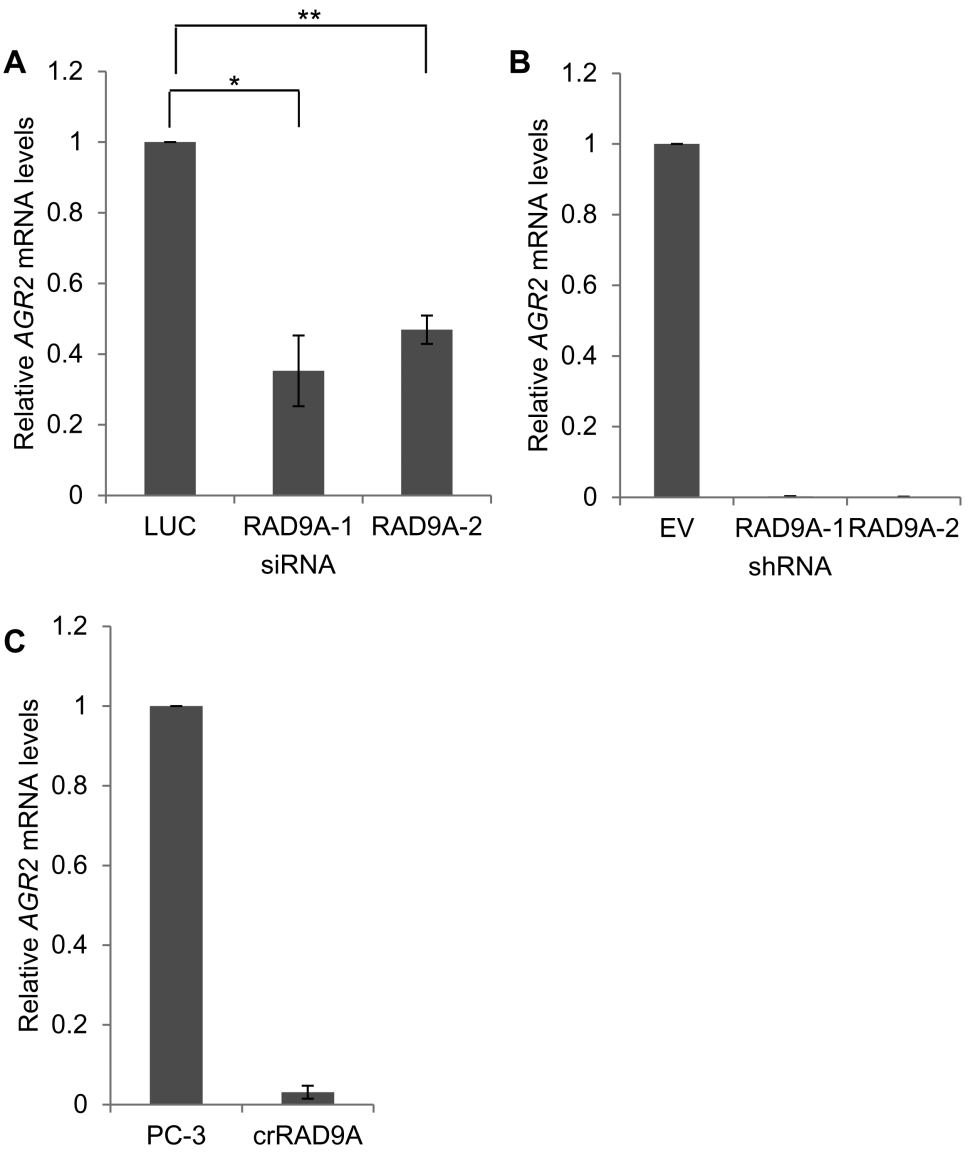

Figure 2. RAD9A silencing impairs *AGR2* expression. (**A**) PC-3 cells were transiently transfected with control (luciferase; *Luc*) or two non-overlapping *RAD9A* siRNAs. Two days post-transfection, total RNA was isolated and *AGR2* mRNA abundance was quantitated by real-time quantitative PCR (RT-qPCR). *GAPDH* transcript abundance served as a control. Data shown as mean ± SD * $P < 0.002$, ** $P = 6.58E\text{-}05$ ($n = 5$) (**B**) PC-3 cells stably transfected with either control (insertless pSUPER-retro vector) or *RAD9A* shRNA (two clones) were examined for *AGR2* mRNA levels by RT-qPCR. Data shown as mean ± SD ($n = 3$). (**C**) Parental PC-3 cells or *RAD9A* knockout PC-3 cells (crRAD9A) were examined for *AGR2* mRNA expression by RT-qPCR. Data shown as mean ± SD ($n = 3$). EV, empty vector.

Ectopic expression of *AGR2* in PC-3/crRAD9A cells partially restores cell migration

We showed previously that knockdown of *RAD9A* in DU145 and PC-3 cells impairs cell migration and invasion (9). Moreover, AGR2 depletion compromises migration of numerous tumor cell lines (25). To examine the effect on migration when *AGR2* is ectopically expressed in PC-3 cells knocked down for *RAD9A* by shRNA, we carried out a wound-healing assay. For the first set of these experiments, PC-3 cells transiently transfected with luciferase (Luc) control siRNA, or siRNA corresponding to *RAD9A* (Rad9A-2) or *AGR2* were used. Figure 5A shows that, relative to the luciferase siRNA control, *RAD9A* siRNA reduced levels of RAD9A and AGR2 proteins, whereas the *AGR2* siRNA only reduced levels of the corresponding protein, as predicted. Furthermore, in agreement with our previous results, knockdown of *RAD9A* impaired cell wound closure. Although in control cells the remaining wound gap was 20% by day 2, in the shRAD9A cell population the wound gap was 75% (Figure 5B). Similarly, *AGR2* knockdown resulted in impaired wound closure with an approximately 65% gap remaining at day 2 (Figure 5B). For the second set of related studies, we used parental PC-3 cells, a derivative knocked out for *RAD9A* (PG13), and two independent clones of the latter ectopically expressing *AGR2* (PG13_AGR2.2, PG13_AGR2.6). The anticipated levels of AGR2, RAD9A and β-actin control proteins in those cells were confirmed by western blotting (Figure 5C). The wound closure assay results for these cells are consistent with the previous study findings (Figure 5B and D). Knockout of *RAD9A* (in PG13 cells) impaired the ability of PC-3 cells to close the wound gap. However, stable ectopic expression of *AGR2* in the cells knocked out for *RAD9A* (PG13_AGR2.2, PG13_AGR2.6) accelerated wound closure. Thus, although the remaining wound gap after 2 days was 77% in *RAD9A* knocked out cells, wound closure accelerated in PG13_AGR2.2 cells with the gap at 58% ($P < 0.03$) and for PG13_AGR2.6 at 46% ($P = 0.002$) (Figure 5D). However, the closure was partial and did not reach the

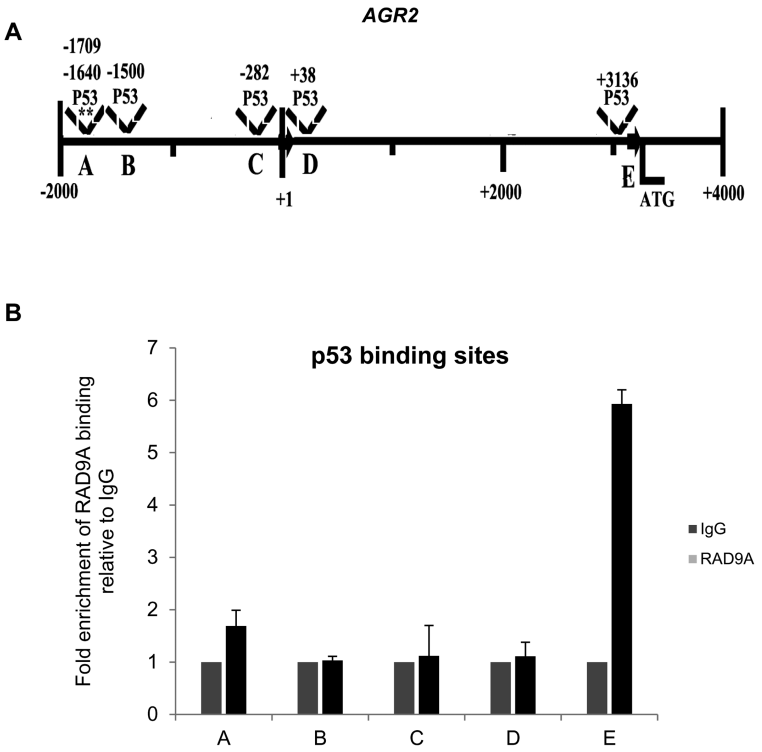

Figure 3. RAD9A protein binds to a p53 consensus sequence at the 5′-untranslated region of *AGR2*. Binding of RAD9A to the putative p53 binding sequences of *AGR2* was tested by ChIP-qPCR using PC-3 cells. (**A**) Schematic representation of P53 binding site positions on the genomic region upstream of human *AGR2*. Each letter represents the primer pair used for ChIP-qPCR. (**B**) Fold enrichment of RAD9A relative to IgG in ChIP-qPCR experiments. Data shown as mean ± SD ($n = 3$). ** = two P53 binding sites.

rate of PC-3 or PC-3/shControl cells. We conclude that AGR2 only partially rescues the migration defect of PC-3/shRAD9A cells and RAD9A affects cell migration by AGR2-dependent and independent pathways.

Ectopic expression of *AGR2* in PC-3/crRAD9A cells restores anchorage-independent growth

Anchorage-independent growth of cancer cells *in vitro* correlates with their ability to produce experimental metastasis *in vivo* (26). We have shown previously that RAD9A depletion in DU145 cells impairs anchorage-independent growth, whereas ectopic expression of mouse *Rad9a* in those cells with depleted endogenous RAD9A is able to restore growth in soft-agarose (9). AGR2 is considered a metastatic gene, and like RAD9A, downregulation of *AGR2* using siRNA impairs anchorage-independent growth in various cancer cell lines (25, 27). In agreement with these results, when *RAD9A* was knocked out in PC-3 cells, they demonstrated reduced ability for anchorage-independent growth, as assessed by colony formation in soft agarose. The cells displayed a 75% reduction in survival compared with parental PC-3 cells (Figure 6A). In contrast, ectopic expression of *AGR2* in PC-3/crRAD9A (clones 2 and 6) cells enhanced their ability to grow in soft-agarose (Figure 6A). Clone 6, expressing elevated AGR2 protein levels compared with clone 2 (Figure 5C), was able to fully reverse the PC-3/crRAD9A cells anchorage-independent growth defect, whereas clone 2 was less effective in doing so. These results support the idea that AGR2 is a downstream effector of RAD9A in the metastatic process.

Discussion

We and others have shown previously that RAD9A protein levels are significantly elevated in a number of human malignancies, including prostate cancer (7). *In vivo* data using xenograft

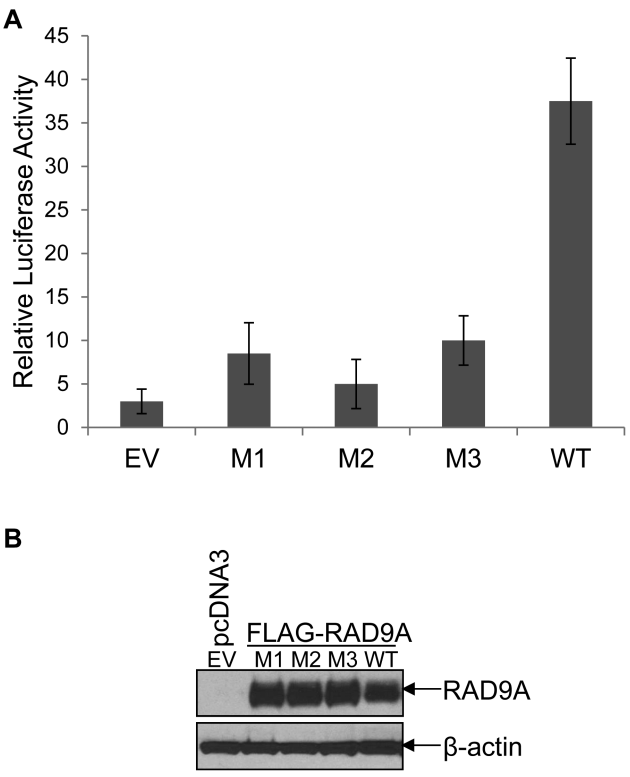

Figure 4. RAD9A functionally controls *AGR2* gene expression. (**A**) Luciferase reporter assay. pcDNA3-RAD9A or pcDNA3 (EV; control) was co-transfected with firefly pGL3-luciferase vector under the control of the wild-type (WT) or three mutated (M1, M2, M3) *AGR2* genomic sequences, together with Renilla pRL-TK, into PC-3 crRAD9 #41 cells. Luciferase activity was normalized by the internal control pRL-TK. Error bars represent the standard deviation of triplicate transfections. (**B**) Western blot analysis of RAD9A protein levels.

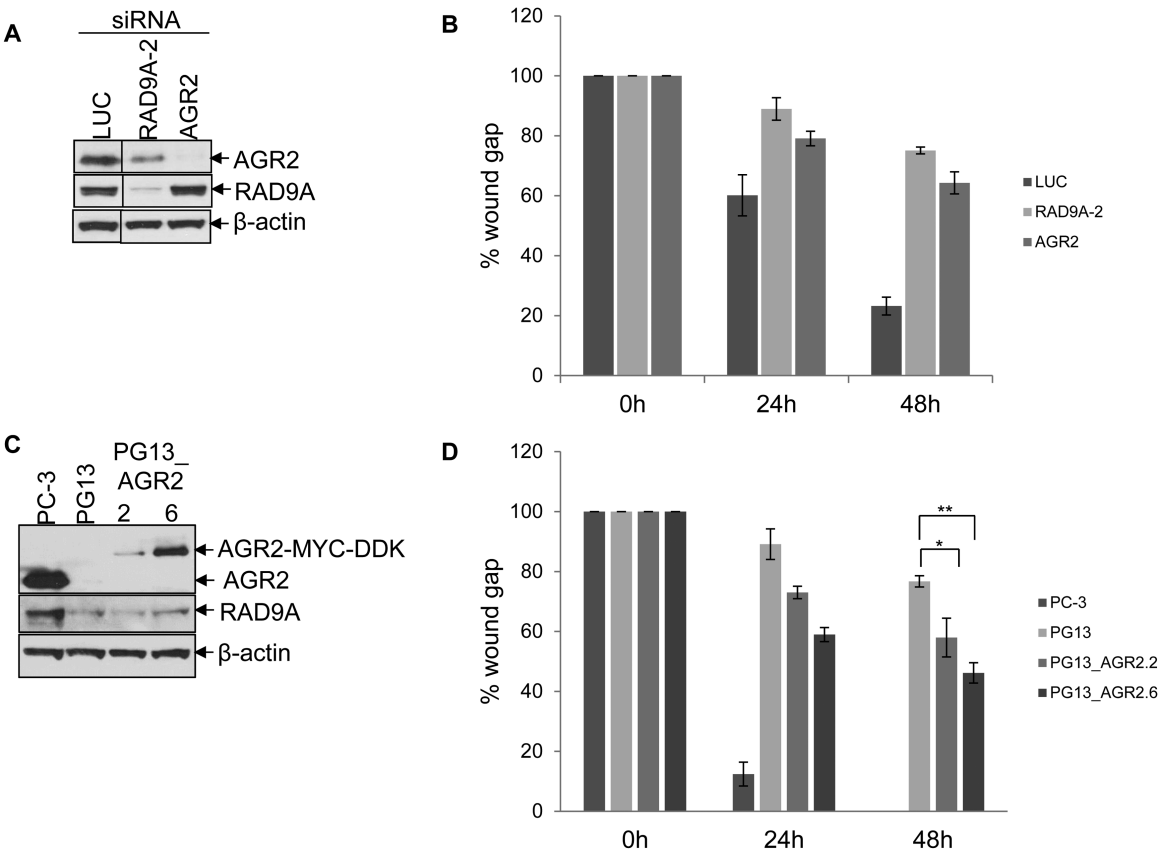

Figure 5. Wound-healing assay. *AGR2* knockdown impairs cell migration. (**A**) PC-3 cells were transiently transfected by siRNA targeting *RAD9A*, *AGR2*, or the Luciferase gene (control), and protein levels were assessed by immunoblotting. (**B**) Wound gap was quantitated at 0, 24 and 48 h after wound placement and removal of dislodged cells from the dish. At time 0 h, values were set at 100%, and wound closure was expressed as a percentage relative to 0 h. Data are mean ± SD (n = 2). Reexpression of *AGR2* partially restores migration capability of PC-3 cells with reduced endogenous levels of RAD9A. (**C**) Western blot analysis showing ectopic expression of FLAG-MYC-tagged AGR2 in PC-3 cells containing low levels of endogenous RAD9A (PG13). (**D**) Wound gap of PC-3 parental cells, PG13 (*RAD9A* targeted using the CRISPR/Cas technology), and two clones of PG13 cells stably expressing ectopic AGR2-MYC-DDK (PG13.2, PG13.6) was quantitated after 0, 24 and 48 h. At time 0 h, values were set at 100%, and wound closure was expressed as a percentage relative to the 0 h. Data are mean ± SD (n = 3). *P < 0.03; **P = 0.002.

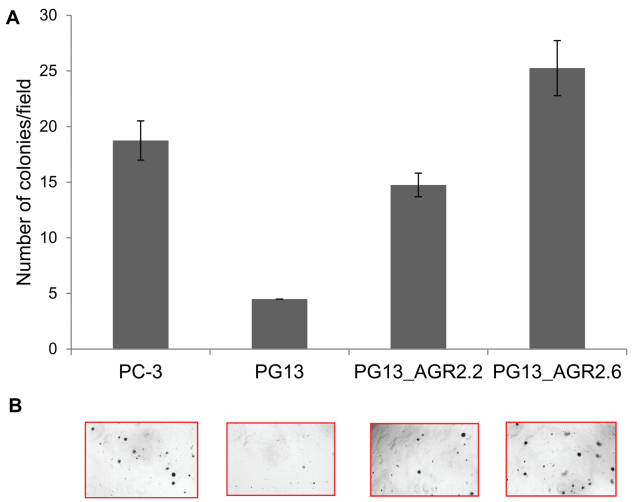

Figure 6. Anchorage-independent growth. (**A**) An equal number of PC-3 cells from different groups was assayed for colony formation in soft agarose. Numbers of colonies with a diameter >20 μm were quantified 3 weeks plating. Shown is one representative experiment of three independent experiments, each performed in triplicate. (**B**) Representative images of colonies in soft agarose.

models have demonstrated that *RAD9A* knockdown in prostate cancer cells impairs their ability to form tumors. Furthermore, immunohistochemical analyses of human prostate cancer specimens revealed that RAD9A is predominantly expressed in more advanced and metastatic stages of prostate cancer (8). However, until recently, mechanistic details of how RAD9A impacts tumor metastasis had been largely unexplored. *RAD9A* silencing in prostate cancer cell lines leads to increased anoikis, impaired cell motility and suppressed anchorage-independent growth, all *in vitro* traits associated with the metastatic process (9). Furthermore, *RAD9A* silencing results in reduced ITGB1 (integrin β1) levels, whereas other integrins are not affected (9, 28). Interestingly, *RAD9A* silencing reduced AKT activation (judged by the reduced phosphorylation levels at Ser473, which is considered a marker for AKT activation) in prostate cancer cells maintained in suspension, but not in cells attached to plastic (9).

RAD9A can act as a sequence-specific transcription factor, a function that is independent of its more established roles in the 9-1-1 complex (4, 5) and in physically interacting with other proteins to repair damaged DNA (3). Interestingly, a number of DNA damage and repair pathway proteins, including BRCA1, PARP1 and TIP60, also function as transcriptional (co)regulators (29). However, whether the DNA damage repair function of these genes is required to promote metastasis or another activity is responsible (e.g., transcription control) has not been determined.

In the current study, we present the novel finding that RAD9A transcriptionally controls the abundance of AGR2. RAD9A binds specifically at a p53-recognition sequence located downstream of the *AGR2* transcriptional start site and induces gene transcription. Other well-characterized p53-responsive genes, such as

PUMA and *DDB2*, have been shown to contain p53 binding sites downstream of their transcriptional start site (30, 31). Although several p53 consensus-like sequences were detected upstream of the *AGR2* protein initiation codon region, RAD9A was able to bind only one of those (at position +3136). The particular nucleotides flanking the p53 consensus sequences, as well as competition with other transcription factors binding at or near the same region could explain this specificity (6). It is known that binding of a transcription factor to a consensus sequence is affected by nucleotide composition flanking the consensus sequence. We found that deleting or mutating the putative binding site abrogates RAD9A binding and transcription. Importantly, RAD9A and AGR2 functionally interact to control migration and anchorage-independent growth. Ectopic expression of *AGR2* in RAD9A-depleted PC-3 cells partially reverses cell migration defects. These results suggest RAD9A regulates cell migration by AGR2-dependent and AGR2-independent mechanisms. A likely AGR2-independent route may be through the activity of ITGB1. We have shown previously that RAD9A is able to modulate levels of ITGB1, an integrin that plays important roles in tumor cell migration (9). Although AGR2 is a regulator of cellular adhesion in prostate cancer and AGR2 knockdown reduces abundance of a number of integrins in PC-3 cells, it does not appear to regulate ITGB1 levels (32). On the other hand, reexpression of AGR2 in PC-3/shRAD9 cells completely rescues the ability of those cells to survive and proliferate under anchorage-independent conditions. These results strongly support a model indicating that RAD9A drives tumor invasion and metastasis by modulating AGR2 abundance.

AGR2 overexpression upregulates numerous genes involved in cell proliferation, migration/invasion and angiogenesis (33), which favor metastasis, and it has been proposed to be a marker that determines negative prognosis in prostate, breast and ovarian cancers. Global gene expression analysis of circulating tumor cells from metastatic carcinomas, including one metastatic prostate cancer revealed that *AGR2* was one of the transcripts consistently detected in CTCs in peripheral blood of advanced cancer patients (34). Furthermore, immunohistochemical staining of AGR2 showed markedly increased expression in high-grade prostatic intraepithelial neoplasia and Gleason stage 3–4 prostatic adenocarcinoma, relative to adjacent benign tissue (16). Overexpression of AGR2 promotes the migration and invasiveness of non-metastatic LNCaP human prostate cancer cells, whereas silencing of AGR2 in metastatic C4-2B cells blocks cell invasion (15). ErbB3 binding protein 1 suppresses AGR2 and impairs metastatic potential in the C4-2B prostate cancer cell line (15). AGR2 promotes migration and invasion of prostate cancer cells (15), but it attenuates cell growth (35).

A number of transcription factors, such as FOXA1/2 (15, 36), FOXM1 (37) and hypoxia-inducing factor 1 (38), function as transcription factors of *AGR2* in various human malignancies. These transcription factors play crucial roles in the advancement of human prostate cancer to castration-resistance and metastasis. FOXA1 pioneer transcription factor is one of the driver oncogenes that lead to castration-resistant prostate cancer (39). Likewise, FOXA2 is involved in progression of prostate cancer to castration resistance (37). Targeting FOXM1 reduces cell growth and stemness in castration-resistant prostate cancer *in vitro* and *in vivo* (40). Finally, HIF1α in cooperation with FOXA2 promotes androgen-independent transition to neuroendocrine prostate tumors (41). However, the particular conditions under which each transcription factor functions, their relative contributions to cancer and the physiological outcome of their activities remain not fully defined.

Future studies in animals will focus on the role of AGR2 in RAD9A-dependent tumor initiation and progression. In this regard, it will be important to evaluate the translational potential of RAD9A and AGR2 as novel diagnostics and therapeutic targets for prostate cancer.

Supplementary material

Supplementary data are available at *Carcinogenesis* online.

Funding

This work was supported by National Institutes of Health grant (CA130536).
Conflict of Interest Statement: None declared.

References

1. Attard, G. *et al.* (2016) Prostate cancer. Lancet, 387, 70–82.
2. Scher, H.I. *et al.* (2015) Prevalence of prostate cancer clinical states and mortality in the United States: estimates using a dynamic progression model. PLoS One, 10, e0139440.
3. Lieberman, H.B. *et al.* (2011) The role of RAD9 in tumorigenesis. J. Mol. Cell Biol., 3, 39–43.
4. Yin, Y. *et al.* (2004) Human RAD9 checkpoint control/proapoptotic protein can activate transcription of p21. Proc. Natl. Acad. Sci. USA., 101, 8864–8869.
5. Panigrahi, S.K. *et al.* (2015) Regulation of NEIL1 protein abundance by RAD9 is important for efficient base excision repair. Nucleic Acids Res., 43, 4531–4546.
6. Lieberman, H.B. *et al.* (2017) p53 and RAD9, the DNA damage response, and regulation of transcription networks. Radiat. Res., 187, 424–432.
7. Broustas, C.G. *et al.* (2012) Contributions of Rad9 to tumorigenesis. J. Cell. Biochem., 113, 742–751.
8. Zhu, A. *et al.* (2008) Rad9 has a functional role in human prostate carcinogenesis. Cancer Res., 68, 1267–1274.
9. Broustas, C.G. *et al.* (2012) Rad9 protein contributes to prostate tumor progression by promoting cell migration and anoikis resistance. J. Biol. Chem., 287, 41324–41333.
10. Chevet, E. *et al.* (2013) Emerging roles for the pro-oncogenic anterior gradient-2 in cancer development. Oncogene, 32, 2499–2509.
11. Brychtova, V. *et al.* (2015) Mechanisms of anterior gradient-2 regulation and function in cancer. Semin. Cancer Biol., 33, 16–24.
12. Bergström, J.H. *et al.* (2014) AGR2, an endoplasmic reticulum protein, is secreted into the gastrointestinal mucus. PLoS One, 9, e104186.
13. Hrstka, R. *et al.* (2016) AGR2 oncoprotein inhibits p38 MAPK and p53 activation through a DUSP10-mediated regulatory pathway. Mol. Oncol., 10, 652–662.
14. Alavi, M. *et al.* (2015) High expression of AGR2 in lung cancer is predictive of poor survival. BMC Cancer, 15, 655.
15. Zhang, Y. *et al.* (2010) ErbB3 binding protein 1 represses metastasis-promoting gene anterior gradient protein 2 in prostate cancer. Cancer Res., 70, 240–248.
16. Zhang, J.S. *et al.* (2005) AGR2, an androgen-inducible secretory protein overexpressed in prostate cancer. Genes. Chromosomes Cancer, 43, 249–259.
17. Fessart, D. *et al.* (2016) Secretion of protein disulphide isomerase AGR2 confers tumorigenic properties. Elife, 5, pii: e13887.
18. Ramachandran, V. *et al.* (2008) Anterior gradient 2 is expressed and secreted during the development of pancreatic cancer and promotes cancer cell survival. Cancer Res., 68, 7811–7818.
19. Vitello, E.A. *et al.* (2016) Cancer-secreted AGR2 induces programmed cell death in normal cells. Oncotarget, 7, 49425–49434.
20. Tohti, M. *et al.* (2017) Serum AGR2 as a useful biomarker for pituitary adenomas. Clin. Neurol. Neurosurg., 154, 19–22.
21. Livak, K.J. *et al.* (2001) Analysis of relative gene expression data using real-time quantitative PCR and the 2(-Delta Delta C(T)) method. Methods, 25, 402–408.

22. Wang, X. *et al.* (2012) PrimerBank: a PCR primer database for quantitative gene expression analysis, 2012 update. Nucleic Acids Res., 40, D1144–D1149.
23. Panigrahi, S.K. *et al.* (2012) Sp1 transcription factor and GATA1 cis-acting elements modulate testis-specific expression of mouse cyclin A1. PLoS One, 7, e47862.
24. Wingender, E. *et al.* (2000) TRANSFAC: an integrated system for gene expression regulation. Nucleic Acids Res., 28, 316–319.
25. Wang, Z. *et al.* (2008) The adenocarcinoma-associated antigen, AGR2, promotes tumor growth, cell migration, and cellular transformation. Cancer Res., 68, 492–497.
26. Cifone, M.A. *et al.* (1980) Correlation of patterns of anchorage-independent growth with *in vivo* behavior of cells from a murine fibrosarcoma. Proc. Natl. Acad. Sci. USA., 77, 1039–1043.
27. Vanderlaag, K.E. *et al.* (2010) Anterior gradient-2 plays a critical role in breast cancer cell growth and survival by modulating cyclin D1, estrogen receptor-alpha and survivin. Breast Cancer Res., 12, R32.
28. Broustas, C.G. *et al.* (2014) RAD9 enhances radioresistance of human prostate cancer cells through regulation of ITGB1 protein levels. Prostate, 74, 1359–1370.
29. Broustas, C.G. *et al.* (2014) DNA damage response genes and the development of cancer metastasis. Radiat. Res., 181, 111–130.
30. Nakano, K. *et al.* (2001) PUMA, a novel proapoptotic gene, is induced by p53. Mol. Cell, 7, 683–694.
31. Tan, T. *et al.* (2002) p53 binds and activates the xeroderma pigmentosum DDB2 gene in humans but not mice. Mol. Cell. Biol., 22, 3247–3254.
32. Chanda, D. *et al.* (2014) Anterior gradient protein-2 is a regulator of cellular adhesion in prostate cancer. PLoS One, 9, e89940.
33. Park, K. *et al.* (2011) AGR2, a mucinous ovarian cancer marker, promotes cell proliferation and migration. Exp. Mol. Med., 43, 91–100.
34. Smirnov, D.A. *et al.* (2005) Global gene expression profiling of circulating tumor cells. Cancer Res., 65, 4993–4997.
35. Bu, H. *et al.* (2011) The anterior gradient 2 (AGR2) gene is overexpressed in prostate cancer and may be useful as a urine sediment marker for prostate cancer detection. Prostate, 71, 575–587.
36. Mirosevich, J. *et al.* (2006) Expression and role of foxa proteins in prostate cancer. Prostate, 66, 1013–1028.
37. Kalin, T.V. *et al.* (2006) Increased levels of the FoxM1 transcription factor accelerate development and progression of prostate carcinomas in both TRAMP and LADY transgenic mice. Cancer Res., 66, 1712–1720.
38. Hong, X.Y. *et al.* (2013) AGR2 expression is regulated by HIF-1 and contributes to growth and angiogenesis of glioblastoma. Cell Biochem. Biophys., 67, 1487–1495.
39. Grasso, C.S. *et al.* (2012) The mutational landscape of lethal castration-resistant prostate cancer. Nature, 487, 239–243.
40. Ketola, K. *et al.* (2017) FOXM1 has been associated with highly aggressive, castration-resistant prostate cancer tumors targeting prostate cancer subtype 1 by forkhead box M1 pathway inhibition. Clin. Cancer Res., 23, 6923–6933.
41. Qi, J. *et al.* (2010) Siah2-dependent concerted activity of HIF and FoxA2 regulates formation of neuroendocrine phenotype and neuroendocrine prostate tumors. Cancer Cell, 18, 23–38.